CP 594

Sensor Alternatives for Future Unmanned Tactical Aircraft

E. L. Fleeman
The Boeing Company
3370 Miraloma Avenue
Anaheim, CA 92803 U.S.A.

SUMMARY

This paper addresses the enabling technologies of the sensor suite for the next generation Unmanned Tactical Aircraft (UTA). An assessment is made of target sensors, communication sensors, and navigation sensors that are used in the UTA intelligence, surveillance, reconnaissance, communication, and target designation missions. Emphasis is given to the classes of UTAs that operate at stand-off altitudes and ranges outside the effectiveness envelope of typical threat air defenses and jammers.

Primary environmental factors that are addressed in the paper are world-wide cloud cover and rain rate. The effects of cloud cover and rain rate on sensor performance are evaluated for synthetic aperture radar (SAR), passive millimeter wave (mmW), and electro-optical (EO) sensors. The synergy of radar frequency (RF) sensors to improve the sensor suite performance in cloud cover and rain rate is addressed.

The paper also addresses the enabling technologies that are required for real time, low false alarm rate (FAR), automatic target recognition (ATR) and precision targeting. A target sensor suite is postulated that is based on multi-spectral, multi-dimension discriminants of the target. An X-band or Ku-band SAR is considered to be the best overall target sensor for UTA applications. A priority ranking of other target sensors is ultra wide band (UWB) low frequency SAR, forward looking infrared (FLIR), laser infrared detection and ranging (LIDAR), visible, and passive mmW. The Year 2007 sensor suite would cover the multi-spectral range of VHF frequency to visible wavelength and the multi-dimensional parameters of contrast, two-dimensional shape, three-dimensional shape, temporal, and polarization signatures of the target.

LIST OF ACRONYMS AND SYMBOLS

	Definition
A/J	Anti-Jam
ADTS	Advanced Detection Technology Sensor
ATR	Automatic Target Recognition
C-band	3.6 GHz to 7.0 GHz
C/A	Course Acquisition
CALCM	Conventional Air Launched Cruise Missile
CARABAS	Coherent All Radio Band Sensing
CCD	Charge Coupled Device
CCM	Counter-Countermeasure
CdZnTe	Cadmium Zinc Telluride
CLO	Counter Low Observable
D	Diameter
dB	Decibel
DQI	Digital Quartz IMU
ERIM	Environmental Research Institute of Michigan
FAR	False Alarm Rate
FM	Frequency Modulation
FMCW	Frequency Modulation Continuous Wavelength
FOG	Fiber Optic Gyro
FOV	Field of View
FPA	Focal Plane Array
GPS	Global Positioning System
HgCdTe	Mercury Cadmium Telluride
Hz	Hertz (cycles per second)
ID	Identification
IFOV	Instantaneous Field-of-View (field-of-view of one resolution cell)
IIR	Imaging Infrared
IMU	Inertial Measurement Unit
INS	Inertial Navigation System
InSb	Indium Antinimide
IR	Infrared
ITCZ	Inter Tropical Convergence Zone
Ka-band	~35 GHz
Ku-band	~17 GHz
LADAR	Laser Detection and Ranging
LIDAR	Laser Infrared Detection and Ranging
LO	Low Observable
LWIR	Long Wave Infrared
MBE	Molecular Beam Epitaxy
mmW	Millimeter Wave
MWIR	Medium Wave Infrared
PACE	Producible Alternative to Cadmium Telluride for Epitaxy
PFM	Pulse Frequency Modulation
P(Y)	Military Code for GPS Receivers
POGO	Precision On-Board GPS Optimization
PtSi	Platinum Silicide
QWIP	Quantum Well Infrared Photodetector
R	Range to Target
RCS	Radar Cross Section
RF	Radar Frequency or Radio Frequency
RLG	Ring Laser Gyro
RSS	Root Sum of the Squares

SAR	Synthetic Aperture Radar
SATCOM	Satellite Communication
SHF-band	Super High Frequency Band
SIGINT	Signal Intelligence
SOTA	State-of-the-Art
SWIR	Short Wave Infrared
TBD	To Be Determined
TESAR	Tactical Endurance Synthetic Aperture Radar
TLE	Target Location Error
TV	Television
UHF-band	Ultra High Frequency Band
URE	User Range Error
UTA	Unmanned Tactical Aircraft
UV	Ultraviolet
VHF-band	Very High Frequency Band
W	Weight
WAGE	Wide Area Guidance Enhancement
W-band	~94 GHz
X-band	~10 GHz
~	Is similar to
μ	Micron (10^{-6} meter)

1. INTRODUCTION/OPERATIONAL TRENDS OF THE YEAR 2007

Until recently, most Unmanned Tactical Aircraft (UTA) used a relatively unsophisticated sensor suite that typically consisted of a FLIR sensor, a television (TV) camera, and a data link. However, the more recent UTAs, such as Predator, are beginning to carry sophisticated sensor payloads, including multiple infrared (IR) sensors and SAR sensors, that broaden the range of missions and mission performance. Improvements in UTA sensor capability are expected to continue into the next generation multi-mission UTAs. Drivers for the next generation UTAs, that will require improved sensor capability, include a broad range of missions, enhanced survivability, wide area/continuous coverage of the target area, real time ATR, low False Alarm Rate (FAR), and real time precision targeting.

Table 1 shows a typical capability of current UTAs compared to a projected typical capability of the year 2007. The General Atomics Predator UTA was selected as an example of recently introduced UTAs. Other UTAs such as Pioneer and Hunter are less sophisticated than Predator, while developmental UTAs such as Global Hawk and Dark Star will be more sophisticated than Predator. The sensor payload of Predator includes an EO sensor suite, a Ku-band SAR sensor, Ku-band and UHF-band satellite communication (SATCOM), a C-band line-of-sight data link, and a Global Positioning System (GPS)/ Inertial Navigation System (INS) navigator.

Table 1. UTA Capability Forecast

	1997 Example (Predator)	2007 Example
Typical UTA Capability		**UTA Concept TBD**
• Mission	• Surveillance, Recce, Comm.	• Add Intel, target designation, comm. relay
• Maximum Flight Altitude	• 8 km	• > 8 km
• Maximum Sensor Slant Range	• 11 km	• > 20 km
• Maximum Flight Duration	• > 24 hours	• > 24 hours
• Maximum Velocity	• 60 m/s	• 300 m/s
• Observables	• Low	• Lower
• Sensor Payload Weight	• 200 kg	• 200 kg
• ATR Latency	• Post-flight Analysis	• Real-time ATR
• ATR FAR	• High (~ 20/km^2)	• Low (<<1/km^2)
• Targeting Accuracy	• 30 m	• 3 m

Next generation sensors will provide real-time ATR and precision targeting

The Predator's EO sensor suite is the Versatron Skyball SA-144/18 Quartet sensor. It consists of a PtSi 512 x 512 MWIR FLIR, a color TV camera with a 10X zoom, a color TV 900 mm camera, and an eyesafe pulsed erbium: glass laser range finder. The diameter of the EO sensor turret is relatively small--35 cm. The turret has precision pointing with a line-of-sight stabilization accuracy of 10 μrad.

The Predator's SAR sensor is the Northrop Grumman (Westinghouse) Tactical Endurance Synthetic Aperture Radar (TESAR). TESAR provides continuous, near real time strip-map transmitted imagery over an 800 meter swath at slant ranges up to 11 km. Maximum data rate is 500,000 pixels per second. The target resolution is 0.3 meters. TESAR weight and power are 80 kg and 1200 watts respectively.

Also shown in Table 1 is a projected capability for a hypothetical UTA introduced in the year 2007. It is anticipated to have a broad range of missions including surveillance, reconnaissance, communication, intelligence gathering of threat electronic emissions, target designation for weapons attacking moving targets, and communication relay. The system flight performance is expected to be greater than present UTAs, with higher velocity, providing a larger area of coverage and faster response in getting to the target area. The current emphasis on reduced observables is expected to continue, with future UTAs having lower observables.

Advancements in sensor capability are expected to include real time ATR, orders of magnitude reduction in FAR, and an order of magnitude improvement in targeting accuracy. The advanced sensors will leverage the current advanced development (category 6.3A funding) activities that are presently under way.

2. ADVERSE WEATHER CONSIDERATIONS IN SENSOR PAYLOAD

Weather is a driving consideration in the selection of a sensor payload suite. Although a UTA usually operates at high altitude above the weather, the sensor suite must be able to see ground targets through adverse weather.

Cloud cover is a particular concern for UTA sensors because clouds are pervasive in the world-wide weather. The global average annual cloud cover is about 61 percent, with an average cloud cover over land of about 52 percent and an average cloud cover over the oceans of about 65 percent. The average annual cloud cover shown in Figure 1 is based on weather observers around the world. It is a composite of averages that vary widely with geographical location, season, and time of day.

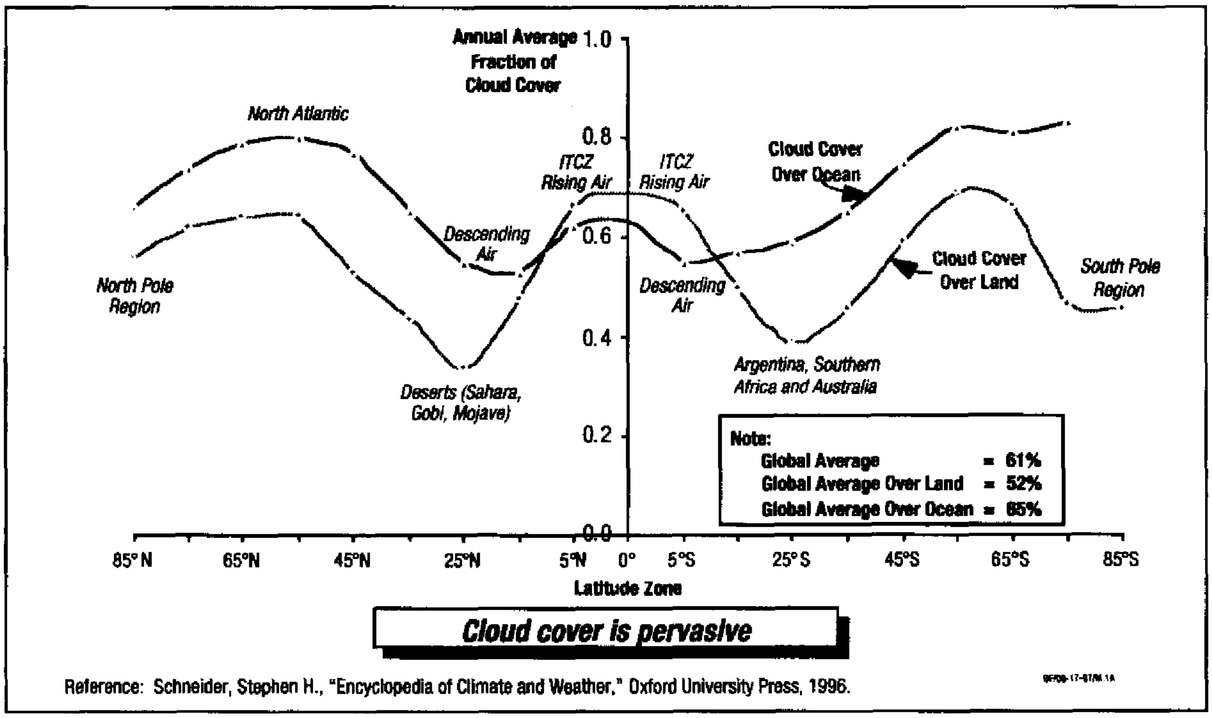

Figure 1. Cloud Cover Climatology

An example of a geographical cloud system that changes regularly with the season and the time of day is the low-level, layered stratus clouds that cover much of the world's oceans. Stratus clouds are more frequent during the summer months of the Eastern Pacific and the Eastern Atlantic and in the hours before sunrise.

Another example of a geographical cloud system that changes regularly with the season and the time of day is cumulonimbus. Cumulonimbus are large columnar clouds that can extend to high altitude. These clouds are concentrated where surface temperatures are high and there is a general upward movement of the air. An example is a zone known as the Intertropical Convergence Zone (ITCZ). In the ITCZ, the trade winds of the Northern Hemisphere converge with those of the Southern Hemisphere. Cumulonimbus have high concentrations of droplets and ice crystals, which can grow to a large size. Cumulonimbus are often responsible for the frequent summer afternoon rainfall of South East Asia, North America, and Europe, and the December, January, and February rainfall of the Amazon basin.

Rain rate is another consideration in sensor selection. Figure 2 shows the world-wide average annual precipitation (rain and snow equivalent rain) characterized as wet (greater than 1500 mm/yr), temperate (between 250 mm/yr and 1500 mm/yr), and arid (less than 250 mm/yr). It is noted that over 90 percent of the world receives less than 1500 mm/yr rainfall. It is also noted that cloud cover variations due to geography, season, and time of day are reflected in the rainfall variations with geography, season, and time of day.

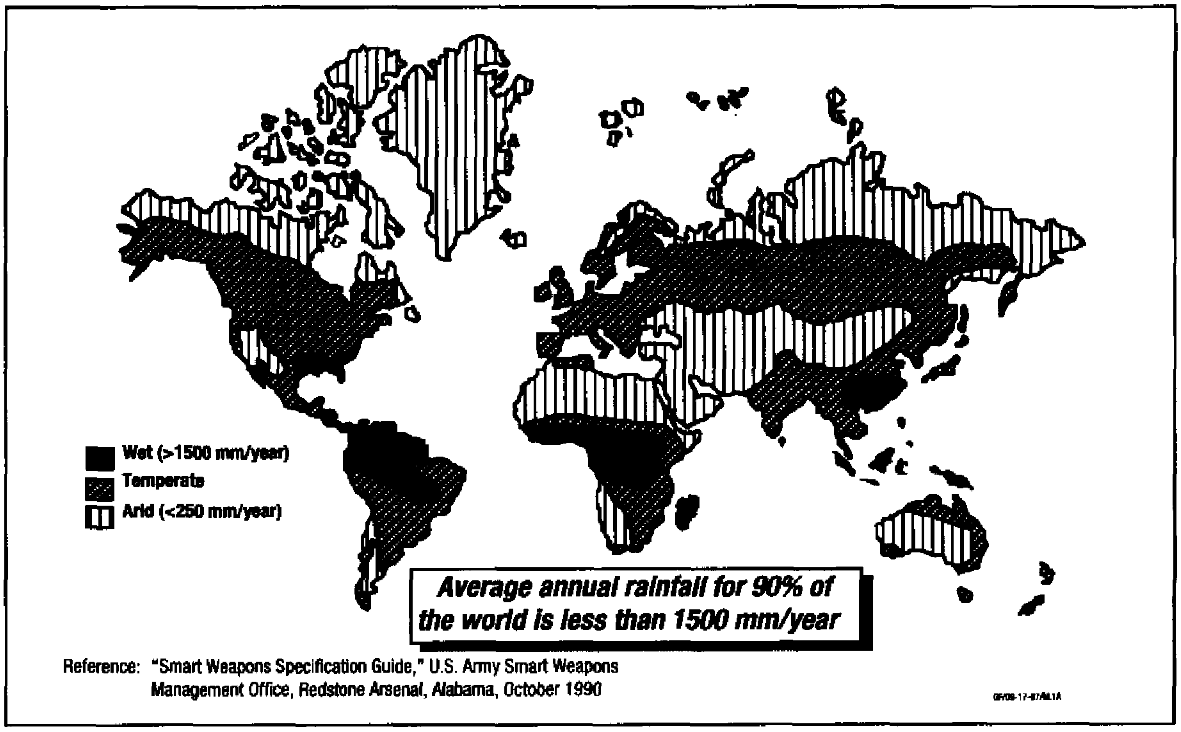

Figure 2. Rain Climatology

UTA sensor attenuation is greater for rainfall from high altitude clouds. There is a longer path length through the rain for high altitude clouds than for low altitude clouds. Figure 3 shows the probability of cloud height for the temperate, wet, and arid regions of the world's land mass. Note that clouds in arid regions tend to occur at higher altitudes while the clouds in the temperate and wet regions tend to occur at lower altitudes. Clouds tend to occur at a height of 1.0 to 5.0 km altitude.

Figure 3 also shows the probability of rain rate for a temperate region of the world that has a relatively high annual rainfall. The average probability of no rain is 80 percent for this region. The probability of rain rate less than 4 mm/hr is very high--96 percent. Also shown for comparison is an average probability of rain rate for the Middle East. The probability of no rain is very high--96 percent and the probability of rain rate less than 4 mm/hr is even higher--99 percent.

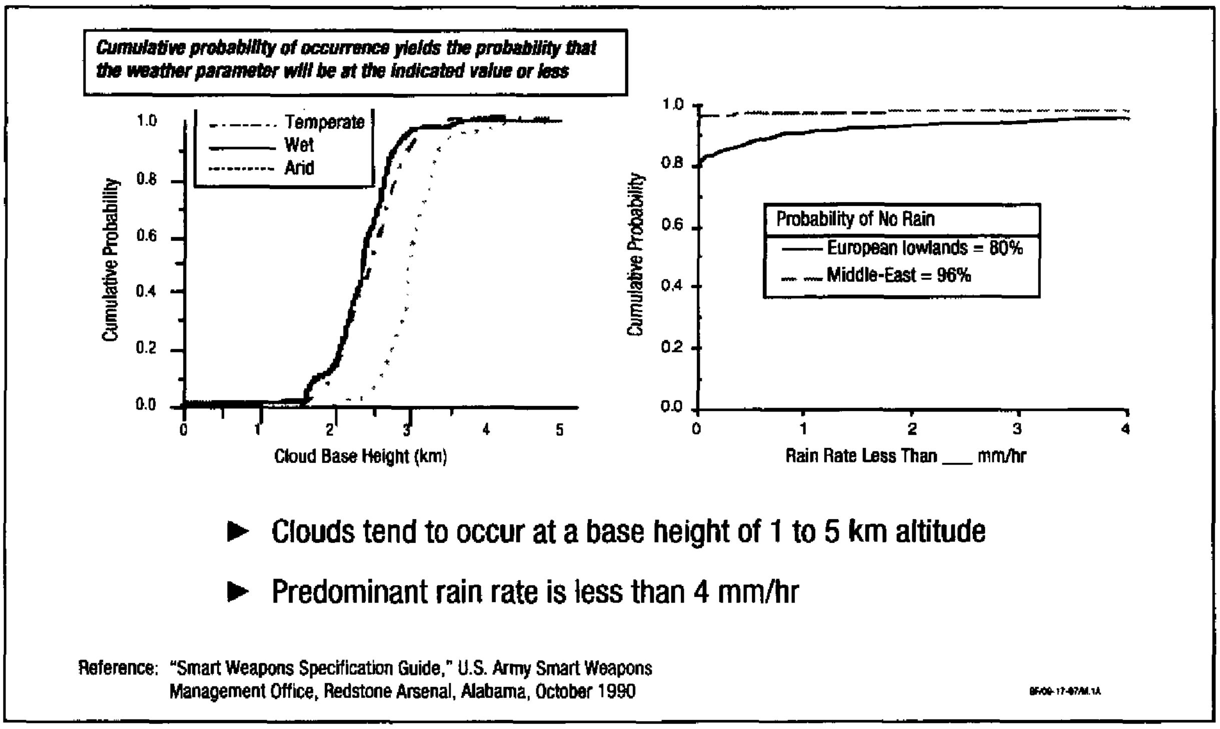

Figure 3. Adverse Weather Performance Requirements

For the purpose of this assessment, a maximum cloud base height of 5 km, a maximum cloud thickness of 2 km, and a rain rate of 4 mm/hr are considered to be cost effective requirements for UTA sensors. It would be unnecessarily restrictive to require UTA sensors to operate in 100 percent weather conditions, such as severe thunderstorms.

Figure 4 shows the attenuation versus wavelength for a representative cloud, rain rate, and humidity level requirement. Note that although passive EO sensors have one-way transmission through rain of about 50 percent per km, there is almost no transmission of an EO signal through clouds. Cloud droplets are small, about 5 to 20 microns in diameter, with dimensions comparable to the EO wavelength. The concentration is high--about 50 to 500 droplets per cubic centimeter. EO wavelengths are strongly diffracted around cloud droplets due to Mie electromagnetic scattering. However, rain drops are about 2-6 mm diameter (much larger than EO wavelengths) and cause less attenuation to an EO signal. Rain rate attenuation is due primarily to optical scattering. EO transmission through rain is a function of the size of the rain drops, rain rate, and the path length through the rain. EO passive sensors are limited from about 2 to 5 km of path length through the rain. The implications of blockage by clouds and the relatively short range in rain are that (1) the UTA will have to descend to low altitude in order to acquire target data using EO sensors, or (2) the UTA will wait for a cloud break to use EO sensors, or (3) use only the radar sensors.

The best sensors in looking down through cloud cover and rain are radar sensors. Radar sensors have negligible attenuation at frequencies below 10 GHz. At higher frequencies, passive millimeter wave sensors operating in cloud cover and rain are limited from about 2 to 5 km length of path through the clouds and rain, with the same implications as those discussed in the previous paragraph. Cloud droplets, which are much smaller than mmW wavelengths, absorb mmW radiation (much like a microwave oven). A different mechanism is responsible for the attenuation of a mmW signal through rain or snow. Rain drops and snow flakes are comparable in size to mmW wavelengths and cause Rayleigh and Mie electromagnetic scattering attenuation. Lower frequency Ku-band sensors are less affected by cloud cover and rain rate.

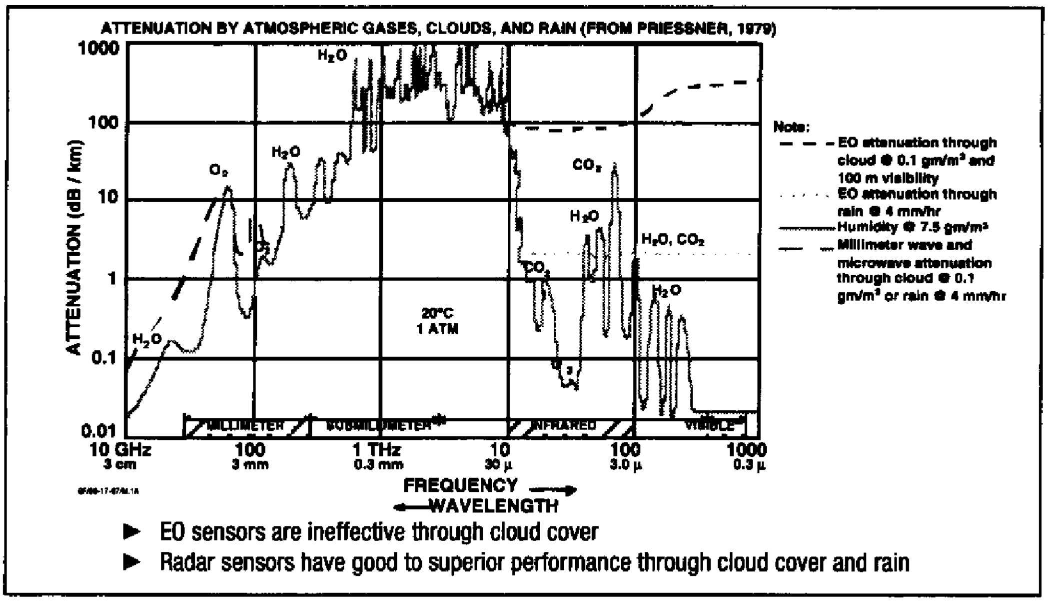

Figure 4. Signal Attenuation Due to Weather

3. SENSOR TECHNOLOGY EXPLOITATION OF THE YEAR 2007

An overall summary comparison of target sensor alternatives against UTA measures of merit is given in Figure 5. The measures of merit selected for the UTA missions are: performance in an adverse weather environment of cloud cover and rain; target resolution capability; contrast of the target to the background clutter; multi-dimensional target discriminants in the areas of polarization, temporal, and shape signatures that are used in ATR; multi-spectral discriminants across a broad range of frequency and wavelength that are used in ATRs; and weight/cost. The adverse weather measures of merit of performance through clouds and rain rate were discussed in Section 2. Figure 5 is based on the assumptions of a cloud thickness of 2 km, a cloud base height of 5 km, and a rain rate of 4 mm/hr.

Sensor Type	Weather: Cloud Cover	Weather: Rain Rate	Resolution	ATR: Contrast	ATR: Polarization	ATR: Temporal	ATR: Shape	ATR: Multi-Spectral	Weight and Cost
SAR	Superior	Superior	Superior	Poor	Superior	Poor	Good	Good	Average
UWB SAR	Superior	Superior	Good	Average	Good	Poor	Average	Superior	Average
FLIR	Poor	Poor	Good	Average	Average	Poor	Good	Superior	Superior
LIDAR	Poor	Poor	Superior	Superior	Poor	Superior	Superior	Good	Good
TV	Poor	Poor	Superior	Poor	Good	Poor	Good	Good	Superior
Passive mmW	Average	Poor	Average	Superior	Poor	Poor	Average	Average	Good
Combined Multi-Spectral, Multi-Dimensional	Superior	Superior	Superior	Superior	Superior	Superior	Superior	Superior	Average

Note: Superior Good Average - Poor

Combined sensors provide superior performance

Figure 5. Target Sensor Suite Performance Projected to Multi-Mission UTAs of the Year 2007

The best overall sensor for a UTA payload is probably a SAR sensor operating at a frequency in either the X-band (~10 GHz) or in the Ku-band (~17 GHz). These bands permit a small antenna size while also providing a capability to penetrate clouds and rain rate. SAR sensors have the flexibility required to cover an area search (e.g., 5 km by 5 km) for single cell target detection, then switch to high resolution (e.g., 0.3 meter) for target ID and targeting. SAR sensors also provide high accuracy profiling of the known terrain features around the target.

Although current SAR sensors have good imagery performance, their current ATR and FAR performance is much worse than the performance of a human. At the present time, SAR sensors require post-flight human analysis of the SAR imagery in order to identify targets and eliminate false alarms. This time consuming process will be alleviated in the next generation ATR that will include polarization discriminants. The additional information will be fused with the SAR imagery as well as information from the other sensors in the UTA sensor suite to greatly enhance ATR.

Polarization provides a SAR sensor with the capability to extract information on the target at long range from a single cell of data. Full polarization algorithms are under development by Boeing. Full polarization (transmit left/right, receive left/right) allows complex targets to be decomposed into elemental scatterers such as dihedrals, trihedrals, cylinders, helix, and dipoles.

The Lincoln Laboratory is also currently developing ATR algorithms based on a different approach to SAR polarization. A high resolution, polarimetric SAR called Advanced Detection Technology Sensor (ADTS) has been developed by Lincoln Laboratory under DARPA sponsorship. ADTS will collect mmW SAR polarimetric data on targets in foliage clutter. The center frequency of ADTS is 33.6 GHz and the bandwidth is 600 MHz.

Another enabling technology that allows incorporation of a SAR sensor into a weight limited UTA is the use of phased array antennas with frequency modulation continuous wavelength (FMCW) as an alternative to a conventional pulse frequency modulation (PFM) SAR. A FMCW SAR sensor requires about one eighth the peak power of a PFM SAR, completely eliminating the high power transmitter chassis. Simplified motion compensation is used which requires one fifteenth the computations--motion compensation primarily occurs in radar hardware using digital synthesis and not in the computer. Also, the lower required output of the FMCW SAR system is spread over the full bandwidth in a relatively long chirp, making a FMCW SAR more difficult to detect by the threat. The net result is a SAR that is about one fourth the weight and cost of a conventional PFM SAR.

Referring back to the Figure 5 summary comparison of UTA sensor alternatives, the next priority sensor is considered to be a low frequency ultra wide band (UWB) SAR sensor for foliage penetration. Low frequency UWB SAR has superior performance in cloud cover and rain rate while providing polarized detection of targets in foliage clutter. An example of current UWB SAR is the Swedish Coherent All Radio Band Sensing (CARABAS) VHF UWB SAR. Another example is the ERIM 200 MHz to 900 MHz UWB SAR. The ERIM UWB SAR is currently in flight test evaluation on a P-3 aircraft. Both radars use polarization.

The use of a UWB SAR to detect underground targets is also being investigated. Penetration depths of 1 to 100 meters are possible for UWB SAR sensors operating at frequencies lower than 100 MHz.

Incorporating a relatively large UWB SAR into a UTA is a design and integration challenge. Approaches include incorporating the antenna into the wing or using a leading or trailing boom as an antenna.

Referring back again to the Figure 5 summary comparison of UTA sensor alternatives, note that a FLIR sensor also complements the baseline SAR sensor. Although a FLIR sensor has no performance in cloud cover, there may be opportunities to revisit the target area if there is a cloud break during the long duration mission. The FLIR sensor provides additional multi-spectral, multi-dimensional information at shorter wavelengths. There is a relatively small increase in the sensor suite cost and weight to incorporate a FLIR sensor.

EO focal plane array sensors cover the wavelength range from ultraviolet (UV) through long wave infrared (LWIR). In the IR wavelengths, there are a number of detector materials available. Most IR FPA detectors are mated to a silicon readout circuit through indium columns, resulting in a sandwich or hybrid sensor. There is a potential problem of a mismatch in the thermal coefficient of expansion since these devices operate at cryogenic temperatures. Large IR FPAs tend to have lower yield than the simpler, more easily produced monolithic silicon based FPAs that are used in visible light TV cameras.

In the SWIR and MWIR wavelengths (1 micron to 5 microns), the leading high performance FPA detectors for post-2007 UTA application are InSb, HgCdTe, and Quantum Well Infrared Photodetector (QWIP) detectors. InSb and HgCdTe FPAs of 640 x 480 size are currently in production. In development are array sizes up to 1024 x 1024 with pitch (detector-to-detector spacing) as small as 18 microns. Figure 6 illustrates the state-of-the-art (SOTA) advancements of Boeing's MWIR HgCdTe FPAs. It is postulated that by the year 2007, HgCdTe MWIR FPAs will be in production in a 2048 x 2048 size with 10 micron pitch-performance, providing resolution that is comparable to that of the present SOTA of TV cameras.

QWIP FPAs are based on stacked thin layers of materials that form quantum wells sensitive to a broad range of MWIR and LWIR wavelengths. Each layer is only a few molecules thick, creating energy subbands where quantum effects respond to the IR incident radiation. QWIP FPAs are produced using molecular beam epitaxy (MBE), a relatively inexpensive process, and have high detector uniformity and yield. Disadvantages are a requirement for cooling down to less than 60 Kelvin and a relatively low quantum efficiency.

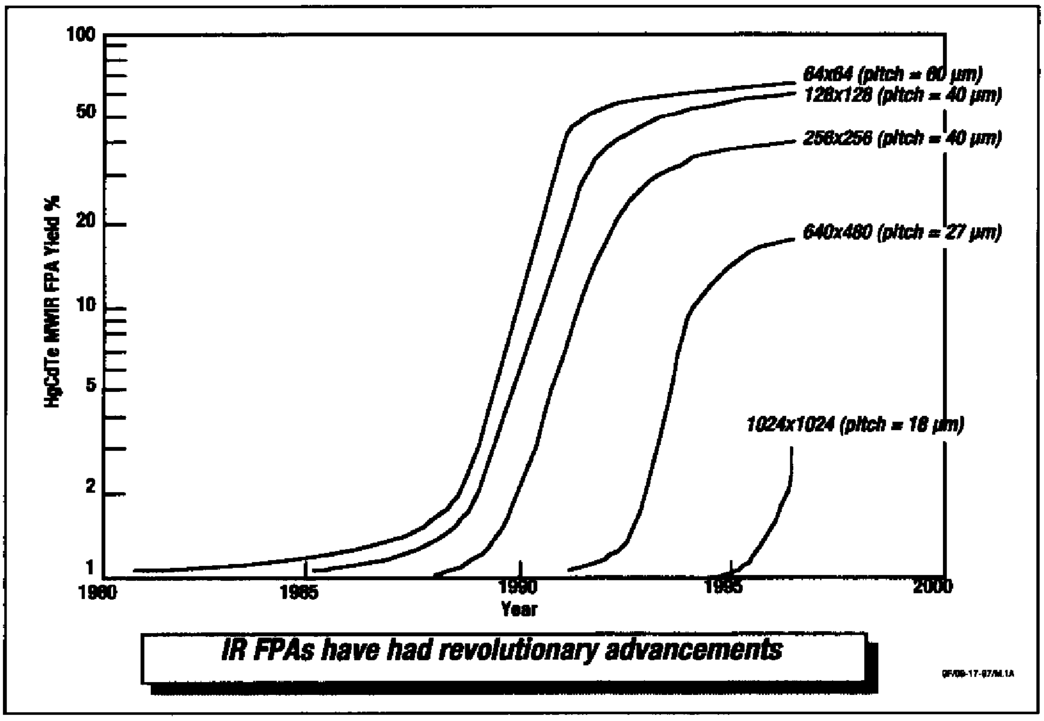

Figure 6. Example of Advancement in SOTA of IR FPAs

LWIR (8 to 12 microns) high performance tactical FPA detectors include HgCdTe and QWIP. HgCdTe LWIR devices that are currently in production have array sizes up to 256 x 256, with a pitch of about 40 microns. It is projected that by the year 2007, HgCdTe LWIR FPAs will be in production in array sizes up to 640 x 480, with 20 micron pitch. It is currently more difficult to produce HgCdTe LWIR FPAs in large array sizes due to the thermal mismatch of the larger LWIR hybrid FPA. Solutions based on a balanced composite structure are currently in development. Also in development are HgCdTe multi-spectral FPAs capable of simultaneous detection in both the LWIR and MWIR bands.

QWIP LWIR FPAs are currently in development. As mentioned in the previous paragraph, QWIP FPAs have advantages of uniformity, low thermal stress even in large size arrays, and suitability for multi-spectral applications. As stated previously, disadvantages of QWIP sensors are a requirement for cooling down to less than 60 Kelvin and relatively low quantum efficiency. Cryo cooler engines operating at temperatures below that of liquid nitrogen (77 Kelvin) are currently in development for application to QWIP FPAs. The relatively low quantum efficiency of QWIP FPAs is expected to be alleviated by technology advancements for this relatively immature technology and the use of multi-spectral discriminants that provide enhanced detection at longer range.

Referring back again to the Figure 5 assessment of UTA sensor alternatives, the fourth priority sensor in an overall sensor suite to detect low observable targets in clutter is Laser Infrared Detection and Ranging (LIDAR), also known as LADAR. LIDAR provides unique three dimensional high resolution and temporal information (e.g., target skin vibration, target exhaust gases) that complement the passive IR sensors of a multi-spectral, multi-dimensional sensor suite. The LIDAR transmitter is usually boresighted to an IR FPA sensor that acquires and tracks the target. The capability to simultaneously measure the passive IR signature and compare it to the reflected LIDAR signature from the laser enhances the ATR performance.

A technology currently in development that will enhance the application of LIDARs is tunable lasers. Tunable LIDARs provide a broader band of wavelength for multi-spectral ATR.

Target designation is a mission that can be addressed by a LIDAR sensor. The UTA sensor suite would hand off target coordinates to the LIDAR for tracking and laser designation. Laser guided weapons launched from manned aircraft platforms would then home on the laser designated target with precision accuracy. It is postulated that UTAs that are designated to carry weapons as part of a primary mission will not occur until after the year 2007 time frame. An operational capability in the year 2007 was used as an assumption in conducting the technology assessment for this paper.

Referring back again to Figure 5, the fifth priority target sensor of a UTA target sensor suite would be a visible light multi-spectral camera. Advantages of a TV sensor include high resolution due to the short wavelength and an additional discriminant of the polarized reflection of sunlight. Although a TV sensor is not effective in cloud cover or at night, a long duration flight UTA could perhaps revisit the target area when appropriate.

Visible detectors are a more mature technology than IR detectors. The detectors are fabricated from silicon, using many of the processes already developed for commercial integrated circuit manufacturing. The visible detector FPA and readout circuitry are usually fabricated in a one piece, monolithic sensor. Large size visible detector arrays are currently in development with array sizes larger than 5000 x 5000. The current SOTA in center detector spacing (pitch) for visible FPAs is 8 to 12 microns.

Referring back to Figure 5 for a final time, note the strengths and weaknesses of passive mmW sensors. Passive mmW sensors have an advantage over EO sensors in their capability to see through cloud cover and the high contrast of metal objects in the mmW spectrum (see Figure 7). Advantages over active RF sensors include lower noise and the avoidance of radar glint. The cold sky (about 35k) is reflected by metal objects at mmW frequencies while the temperature of terrestrial object clutter is about 300k. Current radiometers can typically detect differences in temperature of 1k and radiometers are in development that will detect differences in temperature of 0.1k, providing a very high signal-to-noise ratio of more than 300 to 1.

Passive mmW cameras similar to video cameras are under development by TRW. Cameras have been ground tested at 60 GHz, 65 GHz, 89 GHz, and 95 GHz frequencies. Array sizes up to 40 x 26 elements have been produced. Apertures that have been produced to date range in diameter from 0.4 meter to 0.6 meter. Frame rate demonstrated to date is 17 Hz. Airborne flight tests are planned in late 1997 to flight demonstrate a passive mmW sensor.

Disadvantages of passive mmW sensors include relatively low resolution compared to EO and SAR sensors and attenuation in cloud cover and rain rate. However, passive mmW technology is relatively immature and future passive mmW sensors of the post-2007 time frame will have distributed apertures for operation as a high resolution interferometer. Distributed apertures consisting of ten or more widely spaced apertures could provide an effective aperture that would be comparable to the wing span of the UTA.

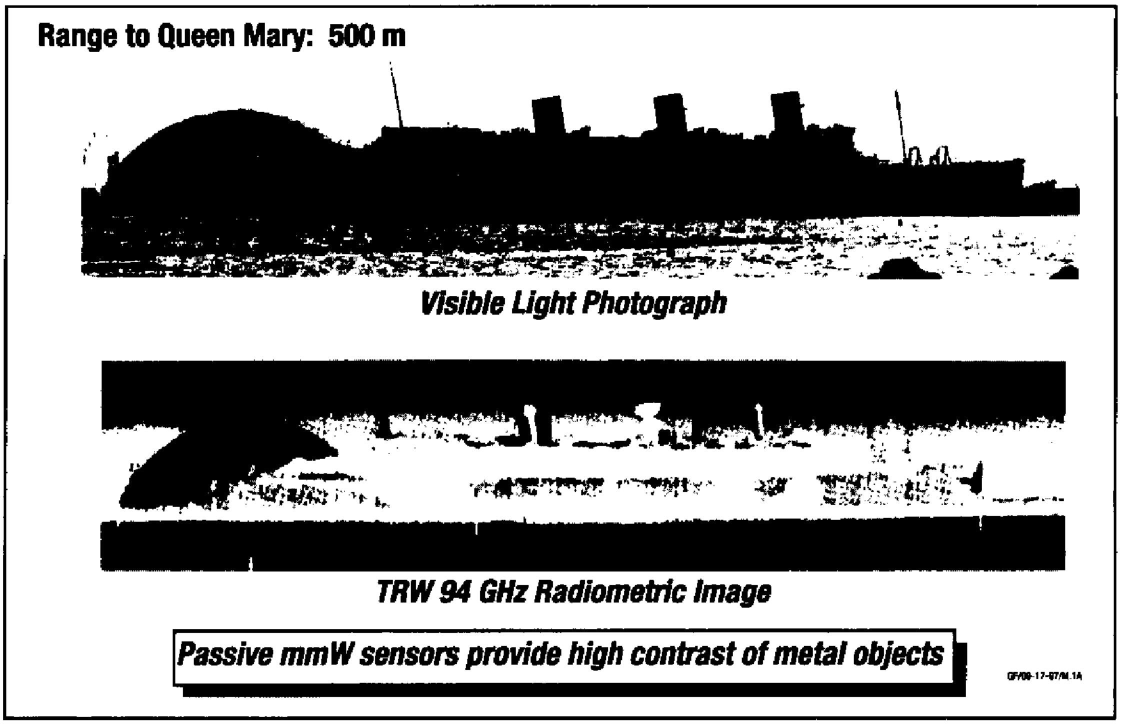

Figure 7. Passive Imaging mmW View of Queen Mary and Spruce Goose Dome

Sensor tracking errors due to the error slope of a conventional hemispherical dome are a traditional problem for EO and RF sensors. Small imperfections in the shape of a hemispherical dome greatly affect the tracking accuracy. An approach that alleviated the problem for EO and RF domes on ballistic missile defense interceptors is to use a flat window as a dome. The error slope of the flat window is nearly negligible compared to a traditional curved hemispherical dome. Another advantage of a flat window for sensors is reduced observables. A grid or slotted film over the window can be tuned to be IR or RF transmissive in the wave length or frequency of interest and RF reflective for out-of-band frequencies. This results in reduced RF back scatter to threat radars, providing reduced radar cross section (RCS) for the UTA. Figure 8 shows experimental and predicted results of the RCS of a treated flat grid pyramidal shaped set of windows compared to a conventional treated hemispherical dome. The 1.5 to 1 length-to-diameter ratio pyramidal flat grid windows provide more than -20 dB reduction in RCS compared to a conventional 0.5 to 1 length-to-diameter ratio hemispherical dome.

As mentioned previously, the current SAR systems generate a tremendous amount of data, driven by requirements for high resolution and large swath widths. The extension of SAR polarization will drive data rates even higher. Communication systems and data links handling capability will need to increase in the future to handle the increased amount of on-board data. Future data transmission systems will use split data links to relay satellites, ground stations, manned aircraft, or other UTAs. UTA data transmission and storage rates SOTA at the present time are of the order of 50 to 100 Megabits per second.

Phased array antennas are in development that provide high data rate (~600 Megabits per second) and flexibility for a UTA to rapidly and efficiently communicate with satellites, ground stations, manned aircraft, or other UTAs. Phased array antennas may also be applicable to agile, highly accurate electronic signal intelligence (SIGINT). A concern in applying phased array antennas to an intel mission is the mission may require operation over a very broad band (e.g., 500 MHz to 35 GHz) that is outside the SOTA of phased array antennas for UTAs.

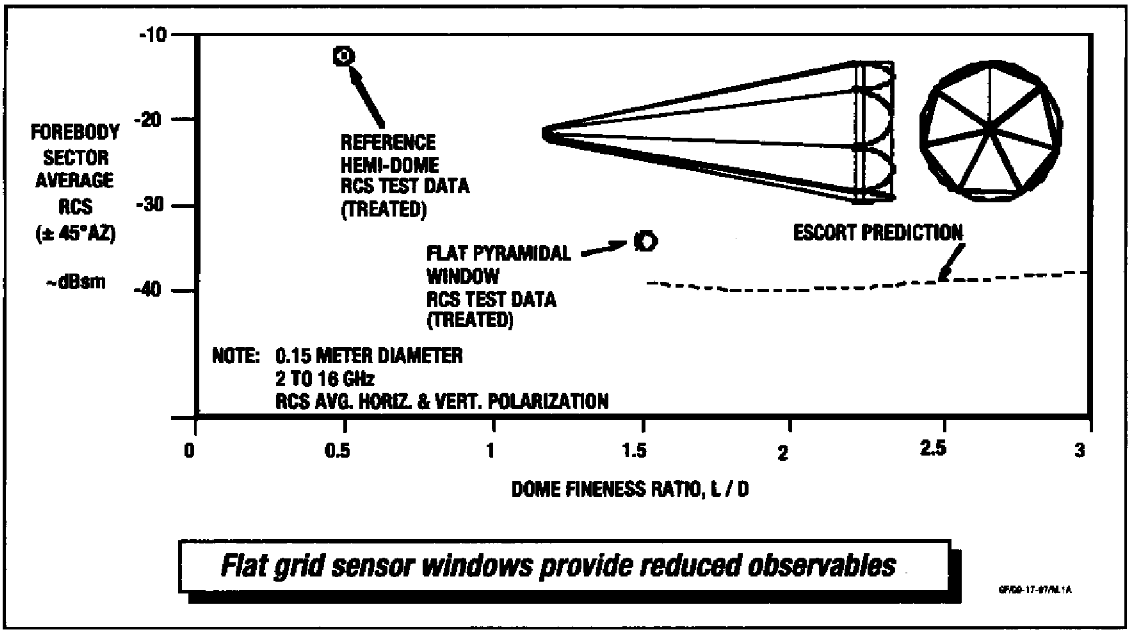

Figure 8. Flat Grid Windows for Sensors

Boeing is developing a family of low cost, high performance phased array antennas for airborne communication (Figure 9). Planar devices have been developed in the SHF-band, Ku-band, and Ka-band. Airborne flight tests have been conducted on military, commercial, and general aviation aircraft.

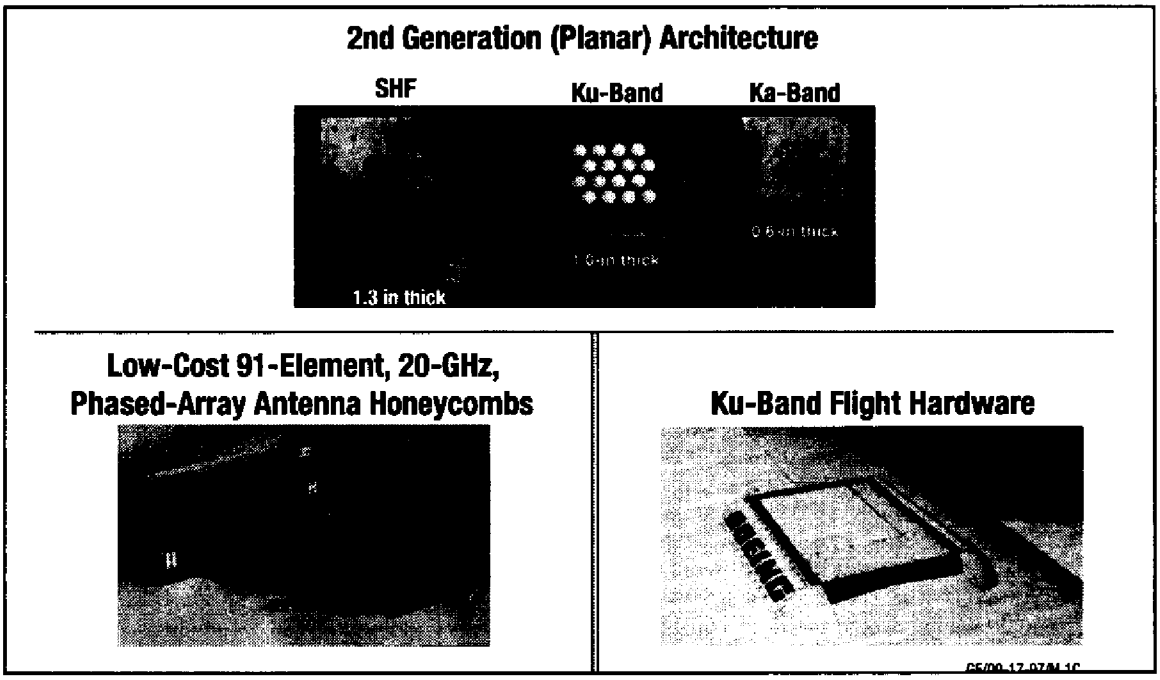

Figure 9. Boeing Phased-Array Family for Mobile Communications

Precision targeting with accuracy better than 3 meters will require high performance navigation sensors. The current Global Positioning System (GPS) receivers operating in a military P(Y) code have an accuracy of approximately 6 meters. Recent advances in using GPS in the Wide Area GPS Enhancement (WAGE) mode, differential mode, or relative mode, combined with SAR precision mapping, have the potential to provide target location with an error less than 3 meters.

Figure 10 illustrates examples of GPS receivers and inertial sensors that are currently being used in GPS/INS navigation. Inertial sensors that are currently available include those based on ring laser gyros, fiber optic gyros, and digital quartz gyros. An emerging technology is a Micromachined Electro-Mechanical Sensor (MEMS) that is fabricated from a single piece of silicon. Good performance is achieved in a small size, low cost package. Between 2,000 and 5,000 devices can be produced on a single five-inch silicon wafer.

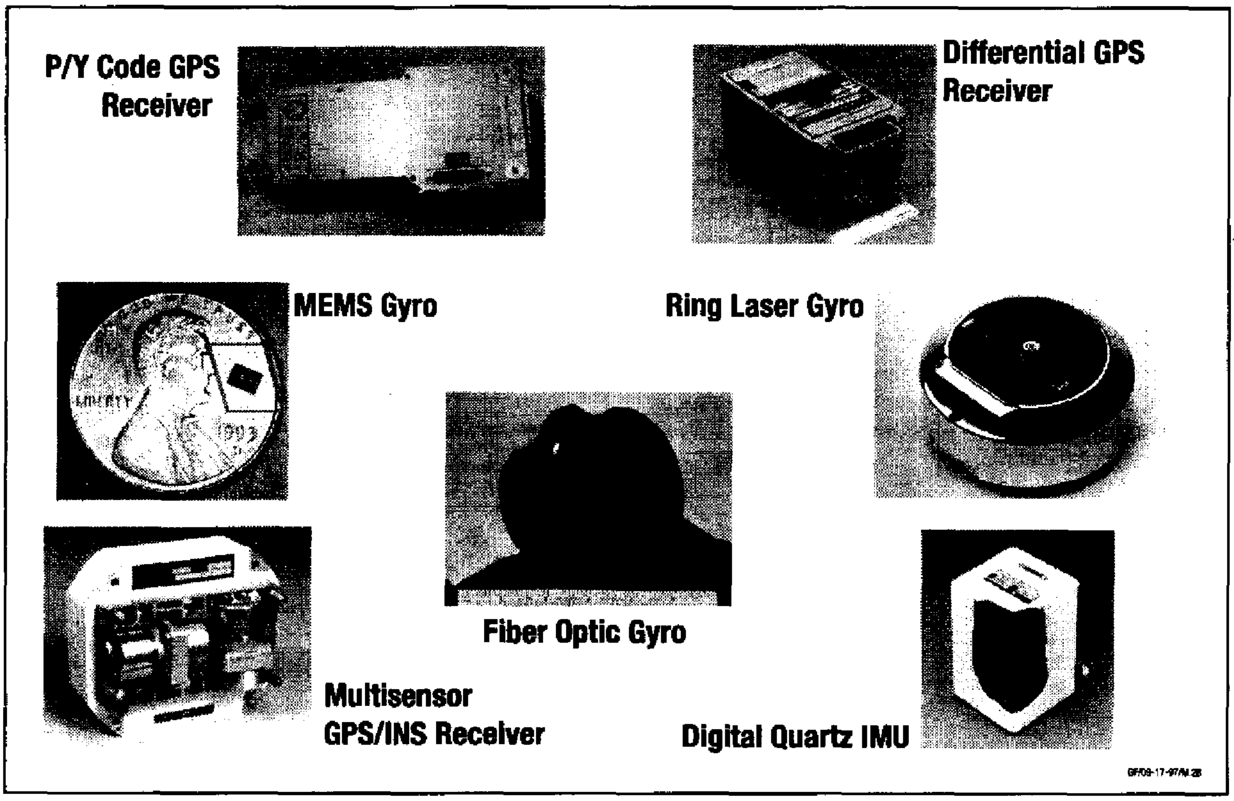

Figure 10. Example of Navigation Sensors

Figure 11 illustrates the advantages of GPS/INS integration. Benefits of GPS/INS integration include high precision position and velocity measurement, reduced sensor noise, reduced jamming susceptibility, and attitude measurement capability. A UTA operating at altitudes higher than 8 km with a modern GPS receiver will have low susceptibility to jamming. The availability of GPS to continuously update the inertial system allows the design trades to consider a lower precision and less expensive INS, while maintaining good navigation accuracy and anti-jam (A/J) performance.

Future GPS/INS receivers will be based on a centralized Kalman filter that processes the raw data from all of the sensors (e.g., SAR, GPS receiver, INS). Tightly coupled GPS/INS is more robust against jamming because it is able to make pseudorange measurements from three, two, or even one satellite if one or more of the satellites are lost.

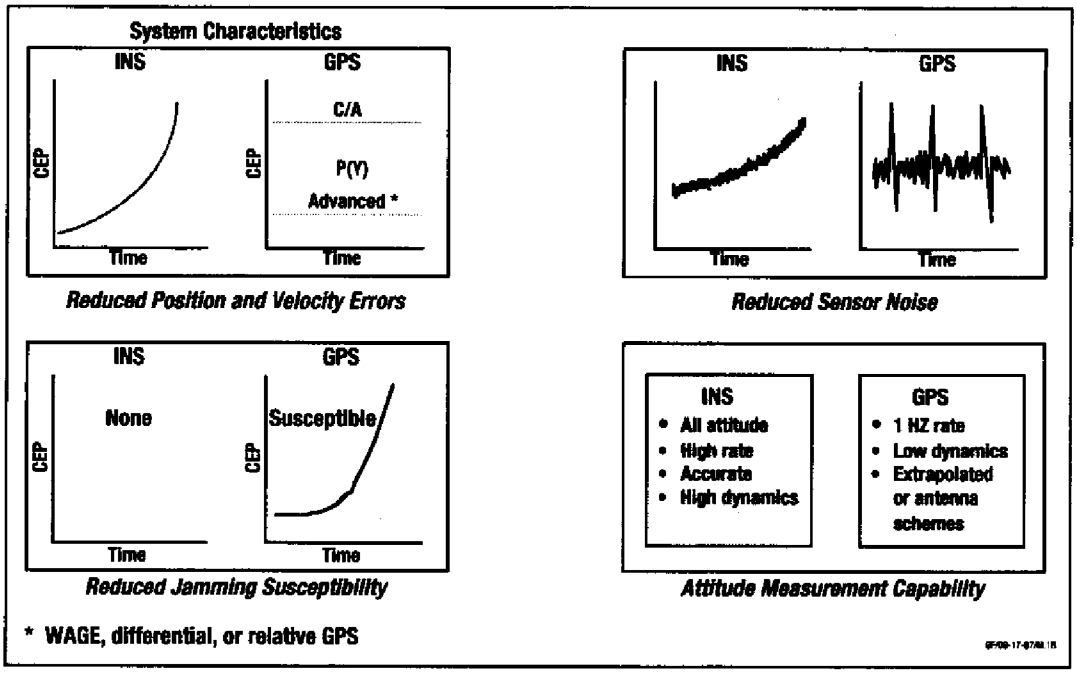

Figure 11. Why GPS/INS Integration?

The 6 meter GPS standard accuracy is improved when multiple GPS measurements are combined in a Kalman filter that provides a calibration of GPS and INS errors. An example shown in Figure 12 is a Conventional Air Launched Cruise Missile (CALCM) demonstration called Precision On-Board GPS Optimization (POGO), where a better than 3 meter accuracy was demonstrated. Ionospheric errors, tropospheric errors, satellite clock errors, satellite ephemeris errors, and other errors were reduced through the use of a centralized sixty state Kalman filter.

Error Sources	Standard GPS	POGO Demo	Source of Improvement
User Range Error	5 m	URE = 2.0M	• WAGE Phase 1
Satellite Ephemeris = 4.0m		1.8	• Accuracy Improvement Initiative (AII)
Satellite Clock = 3.0 m		1.0	• WAGE - complete
		1.0	• Block IIR satellites
Ionosphere	2.3	1.0	• Dual-frequency Receiver • Special algorithm based on phase
Troposphere	2.0	0.5	• Real-time pressure and temperature measurements • Accurate modeling
Multipath	1.2	0.4	• Low missile multipath • Phase use as well as code
GPS Receiver	1.5	0.5	• New technology
RSS Total	***6.2M***	***1.66 - 2.4M***	• URE dependent

URE = User Range Error

Advanced GPS provides precision navigation for targeting

Figure 12. CALCM Precision On-Board GPS Optimization (POGO) Demonstration

A final enabling technology for UTA sensors is sensor electronics. Figure 13 illustrates the rapid growth in electronics for FPAs. The exponential growth in micro processor transistors for FPAs has about a three-year lead on the number of pixels available in IR FPAs and about a four-year lag on the number of pixels available in visible FPAs. There is no sign that the growth rate will slow down. Similar results also apply to memory chips, for example, 256 Megabit dynamic ram memory chips are currently in development

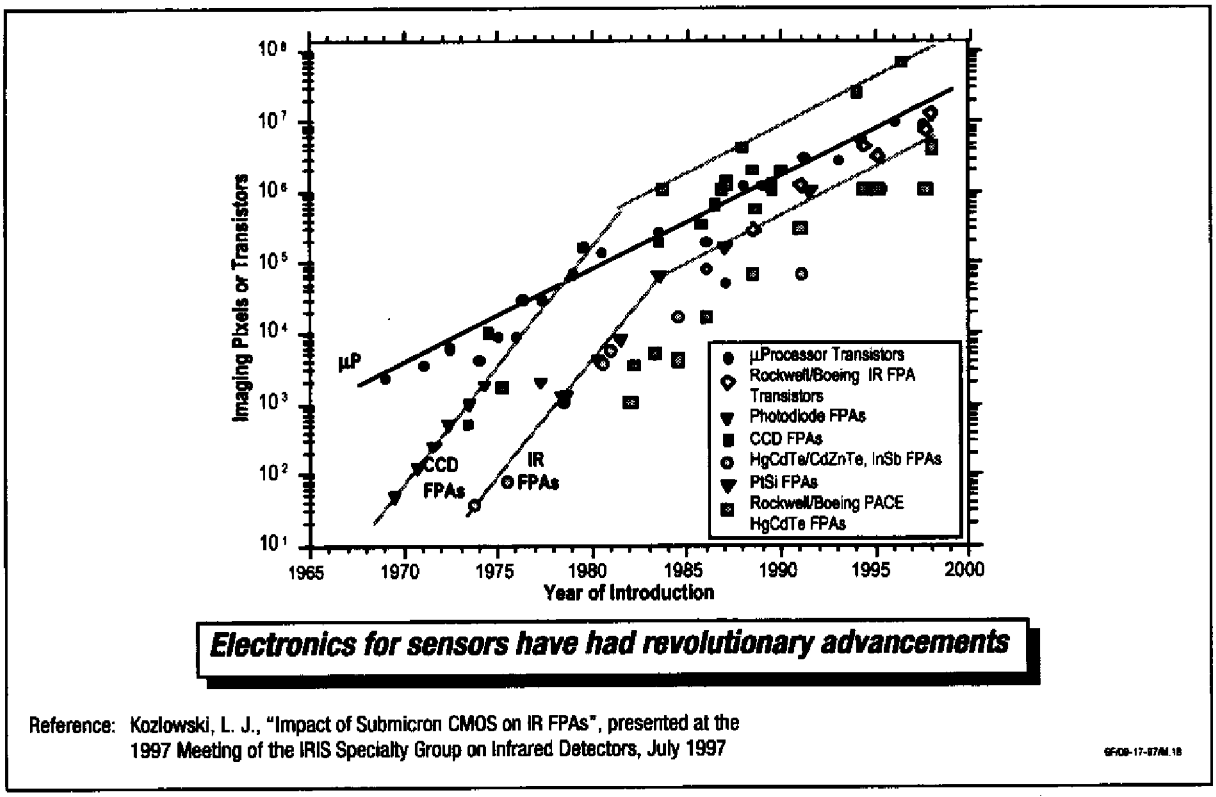

Figure 13. Example of High-Speed, Lightweight Electronics Trend for EO Sensors

4. CONCLUSIONS

Enabling capabilities, performance enhancements, and enabling technologies have been identified for UTAs in the year 2007 time frame. The sensor related enabling capabilities and performance enhancements are:

- Multi-spectral, multi-dimensional sensors that provide real time, low FAR ATR and real time, precision targeting
- Flat windows that provide reduced observables

The sensor enabling technologies are:

- Polarized FMCW SAR sensors for detection, ID and targeting of low observable targets in clutter
- Low frequency, polarized UWB SAR sensors for detection, ID and targeting of low observable targets in foliage
- High resolution, multi-spectral FLIR sensors for ID of low observable targets in clutter
- Tunable multi-spectral, three dimensional, temporal LIDAR sensors for ID and targeting of low observable targets in clutter
- High resolution, multi-spectral visible sensors for ID of low observable targets in clutter
- Moderate resolution, high contrast passive mmW sensors for ID of low observable targets in clutter
- Flat grid windows for reduced observables and low error slope
- Phased array antennas for high agility, high data rate comm
- Agile, broad band, high accuracy electronic SIGINT
- Precision GPS/INS navigation and targeting
- High speed, light weight electronics

5. REFERENCES

Schneider, Stephen H., "Encyclopedia of Climate and Weather," Oxford University Press, 1996.

"Smart Weapons Specification Guide," U.S. Army - Smart Weapons Management Office, Redstone Arsenal, Alabama, October 1990.

Priessner, 1979

U.S. Air Force Science Advisory Board Sensors Panel, "New World Vistas Air and Space Power for the 21st Century - Sensors Volume," 1996.

Kozlowski, L. J., "Impact of Submicron CMOS on IR FPAs," presented at the 1997 Meeting of the IRIS Specialty Group on Infrared Detectors, July 1997.